Electronic Supplementary Material (ESI) for RSC Medicinal Chemistry.

Supporting Information

Synthesis of a Fluorinated Pyronin that Enables Blue Light to Rapidly Depolarize Mitochondria

Zhe Gao,[§] Krishna K. Sharma,[§] Angelo E. Andres, [§]Brandon Walls,[†] Fadel Boumelhem,[†]

Zachary R. Woydziak,[†] and Blake R. Peterson[*§]

[§] Division of Medicinal Chemistry and Pharmacognosy, The Ohio State University, Columbus, OH 43210, USA

[†] Department of Physical and Life Sciences, Nevada State College, Henderson, NV, 89002, USA

Table of Contents **Page(s)**

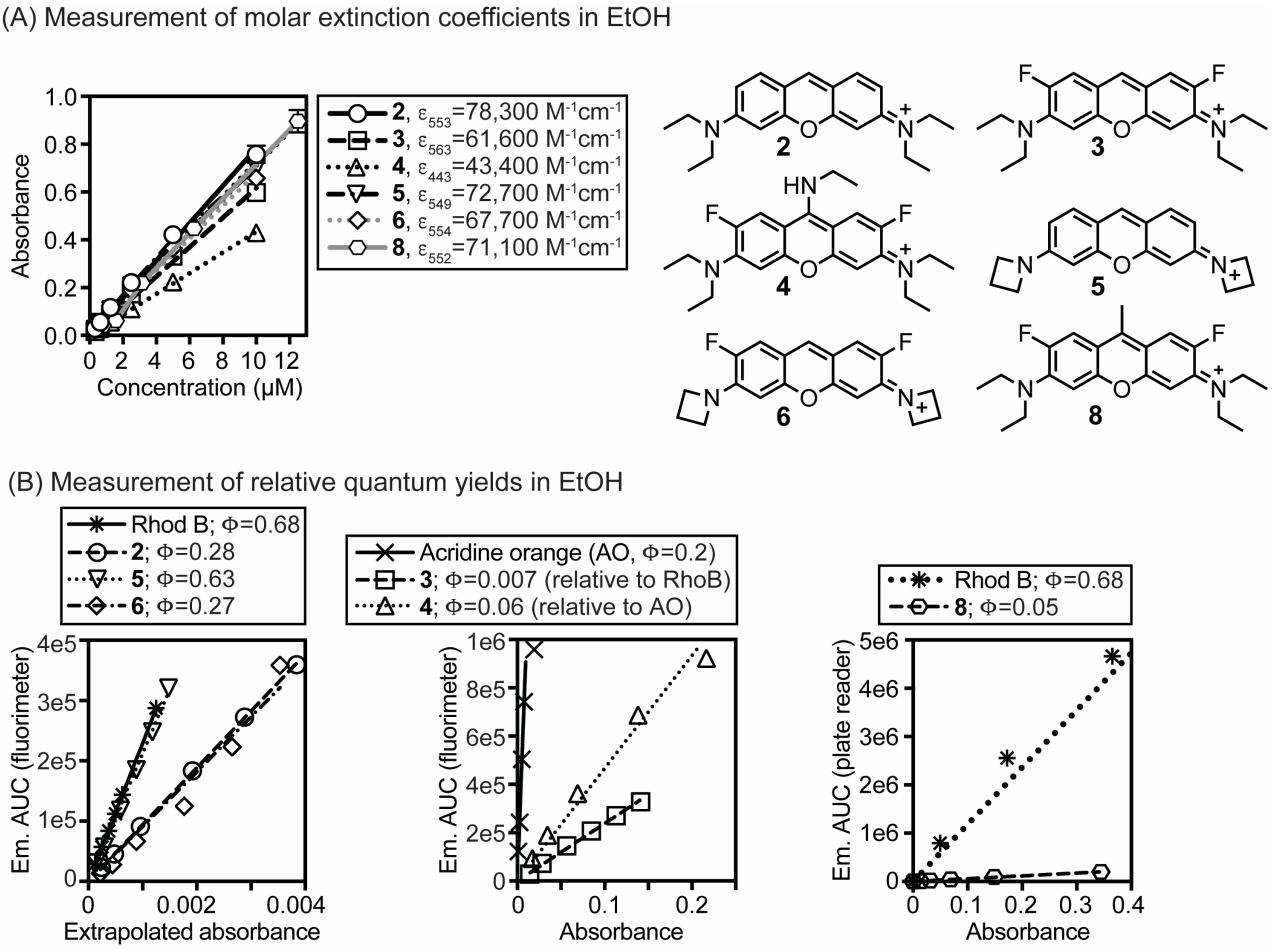

Figure S1. Measurements of molar extinction coefficients (A) and relative quantum yields (B) in EtOH. Standards for determination of relative quantum yields: rhodamine B (Ex. 535 nm) in ethanol for **2**, **3**, **5**, **6**, and **8** (Ex. 535 nm); acridine orange (Ex. 430 nm) in basic ethanol for **4** (Ex. 430 nm). Compound **2** was analyzed as the HCl salt. Compounds **3**–**6**, **8** were analyzed as TFA salts.

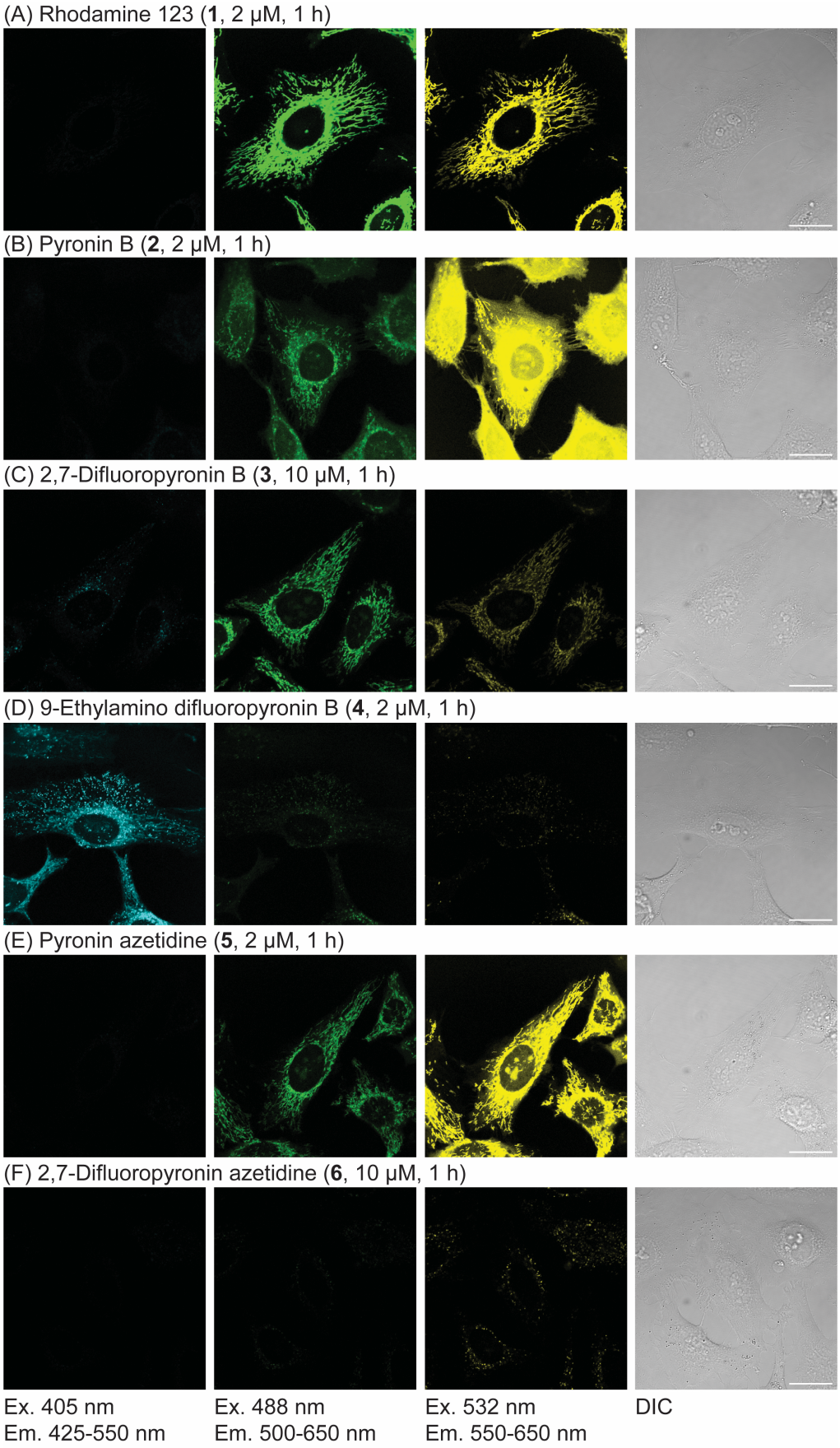

Figure S2. Confocal fluorescence and DIC micrographs of living HeLa cells treated with **1**–**6**. Cells were washed with complete media prior to imaging. Scale bar = 25 μm.

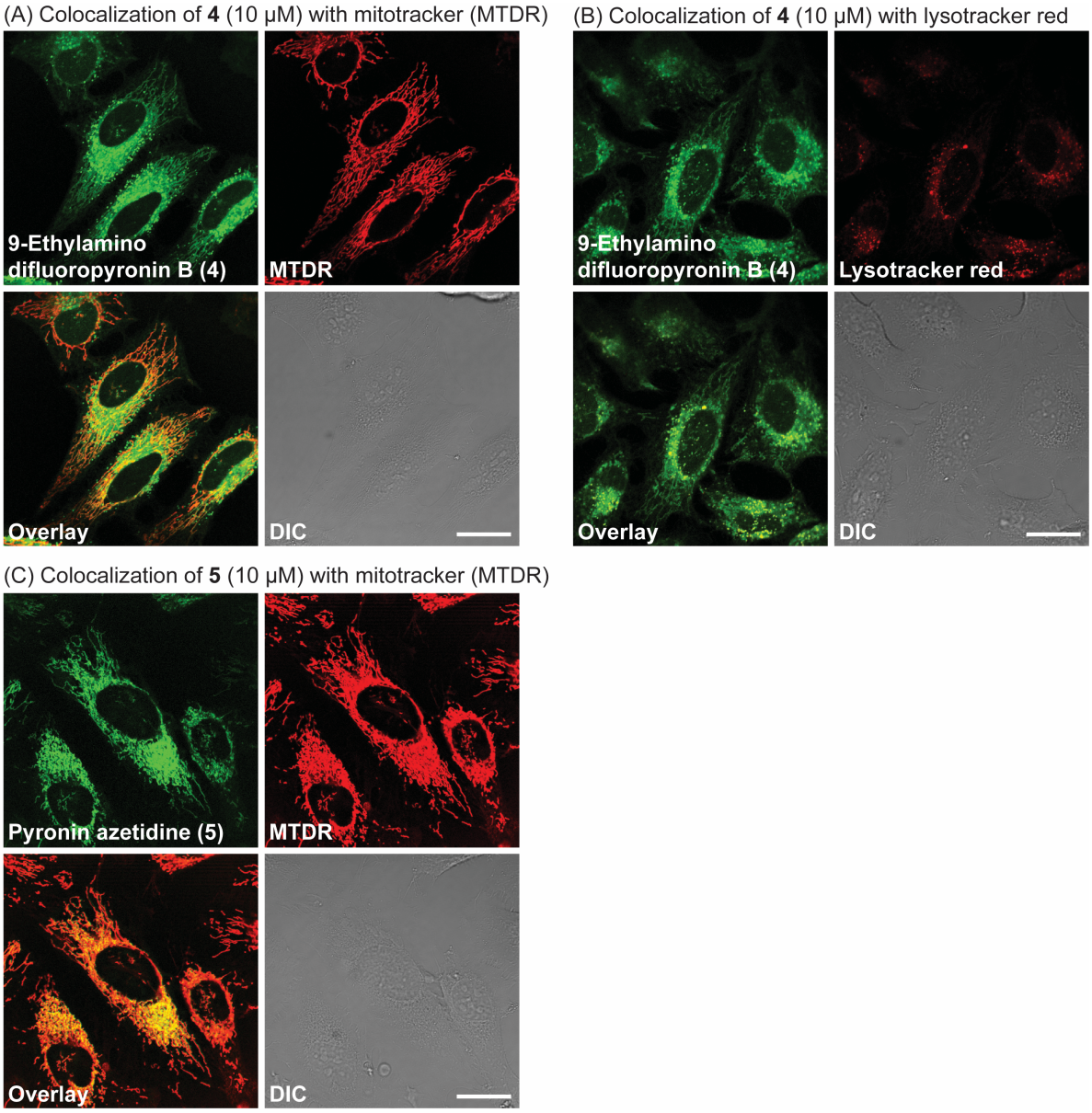

Figure S3. Imaging of colocalization of probes **4** and **5** with organelle markers in living HeLa cells by confocal microscopy. (A) Colocalization of **4** with mitotracker deep red. (B) Colocalization of **4** with lysotracker red. (C) Colocalization of **5** with mitotracker deep red. Cells were imaged without washing. Scale bar = 25 μm.

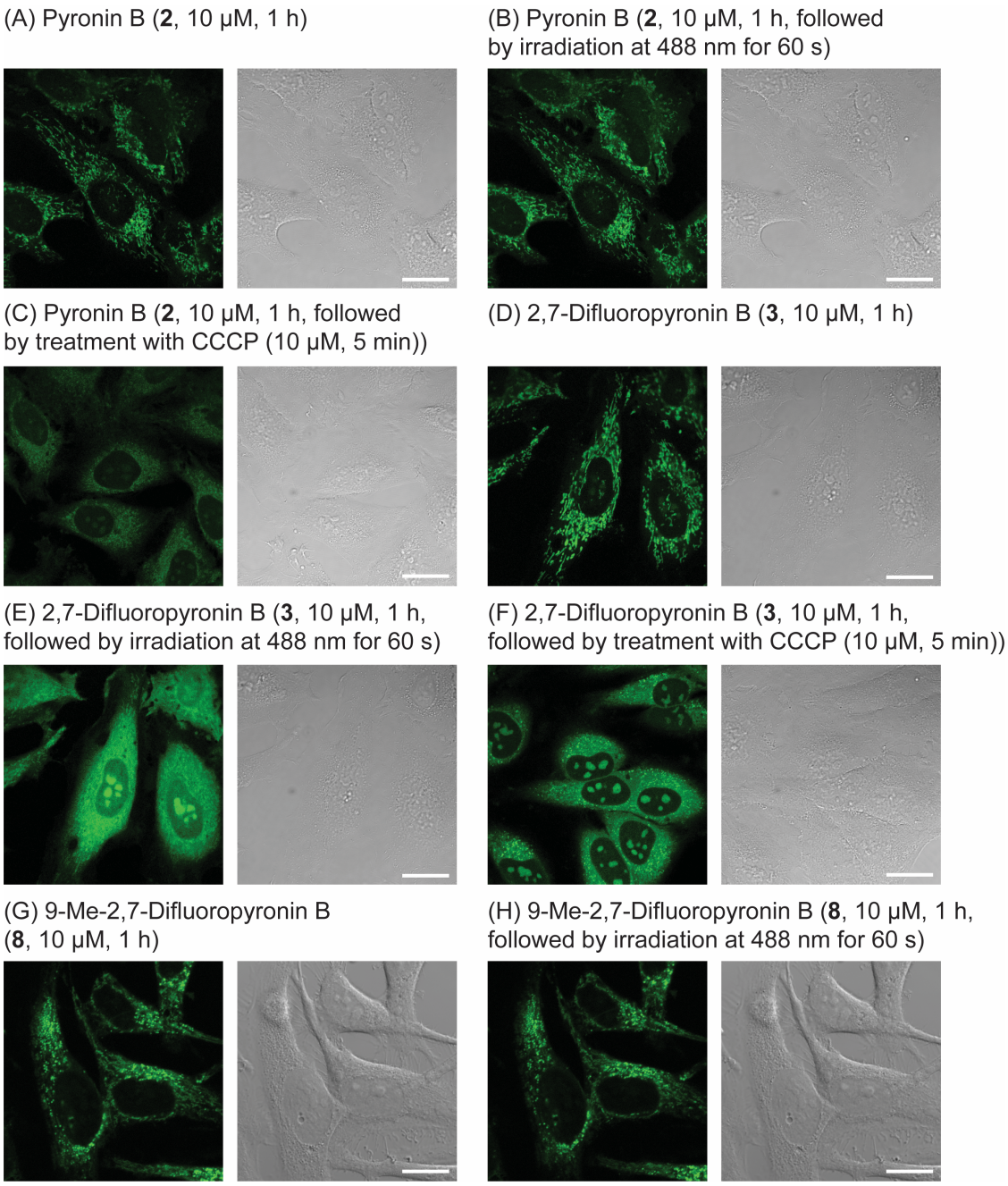

Figure S4. Effects of blue light and the mitochondrial decoupler CCCP on the fluorescence of **2**, **3** and **8** in living HeLa cells. Probe **3** uniquely promoted mitochondrial depolarization upon irradiation. This depolarization phenotype was similar to cells treated with **2** or **3** with subsequent addition of the mitochondrial uncoupler CCCP. HeLa cells were imaged by confocal (left) and DIC (right) microscopy without washing (Ex. 488 nm, Em. 500–600 nm). Scale bars = 25 μm.

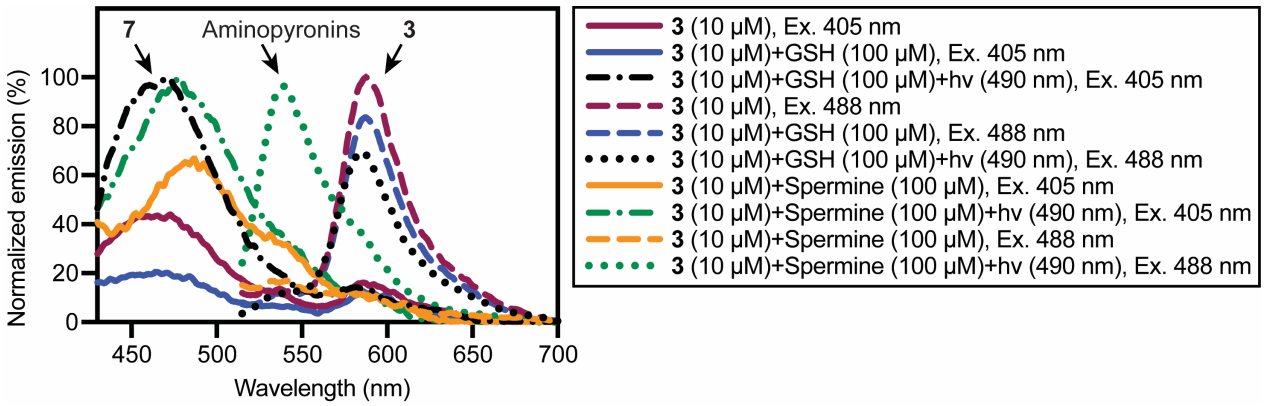

Figure S5. Reactivity of **3** (10 μM) with GSH (100 μM) or spermine (100 μM) in pure unbuffered water at room temperature (22 °C). Compounds were mixed in a cuvette for 1 h and analyzed by fluorescence spectroscopy with excitation at 405 nm or 488 nm. hv = additional irradiation of the cuvette for 10 min with a blue LED flashlight (490 nm). Values are normalized to the maximal emission observed upon excitation at the wavelengths shown. Reaction of **3** and spermine was the most efficient at producing 9-aminopyronins (Em. ~ 540 nm) upon irradiation, but these products are readily hydrolyzed to afford xanthone **7** (Em. ~ 450 nm), which was observed with both spermine and GSH.

Determination of molar extinction coefficients and quantum yields

Molar extinction coefficients (ε) were calculated using Beer's Law: $A = \varepsilon bc$ (A is absorbance, b is path length (typically 1 cm) and c is the concentration). Absorbance spectra were obtained on an Agilent 8453 spectrometer or BMG Labtech ClarioStar plate reader from solutions of dry powders, and maximal absorbance versus concentration was analyzed by linear regression (including a zero intercept) with GraphPad Prism 9 software (slope = ε).

Relative quantum yields (Φ_F) were calculated as: $Q_x = Q_R \times \frac{A_R}{A_x} \times \frac{E_x}{E_R}$, where Q is the quantum yield, A is the absorbance an E is the area under curve (AUC) of the emission spectra. Subscripts X and R refer to the sample and reference compound (Rhodamine B or Acridine Orange), respectively. For highly fluorescent compounds, the absorbance was extrapolated to calculate values at low concentrations. Emission spectra were obtained with a Perkin Elmer LS-55 fluorescence spectrometer or BMG Labtech ClarioStar plate reader, and emission AUC values were calculated with GraphPad Prism 9. Extrapolated absorbance was plotted versus AUC and fitted by linear regression to provide the slope as $\frac{Ex}{Ax}$ of the tested compound. The reference compound provided $\frac{A_R}{E_R}$.

Biological assays and protocols

Cell culture: HeLa cells (CCL-2) were purchased from ATCC, and cultured in Dulbecco's Modified Eagle Medium (DMEM, Sigma D6429). Jurkat lymphocytes (TIB152) were obtained from ATCC and cultured in RPMI-1640 medium (Sigma R8758). Media was supplemented with fetal bovine serum (FBS, 10%, Fisher Scientific, NC0924828), penicillin (100 units/mL), and streptomycin (100 µg/mL, Sigma P4333). Cells were maintained in a humidified 5% CO_2 incubator at 37 °C.

Confocal microscopy: Cells were added to an 8-well chambered coverslip (Ibidi IbiTreat µ-Slide, 300 µL, 20,000 cells/well) and allowed to proliferate for 24 h prior to addition of compounds. Compounds in DMSO stock solutions were serially diluted 1,000-fold in complete medium (final concentration of 0.1% DMSO) prior to addition to cells. Cells were treated with compounds at 37 °C for indicated length of time before imaging with a Leica SPE2 or Leica SP8 confocal laser-scanning microscope (63X oil-immersion objective).

Flow cytometry: Cells were analyzed with a Beckman Coulter Cytoflex S (B2-R0-V2-Y2) flow cytometer. Fluorophores were excited with 405 nm or 488 nm diode lasers and emitted photons were collected through 450/45 nm BP, 525/40 nm BP, or 690/50 nm BP (PI) filters (FSC threshold = 500,000, flow speed = fast, mixing time = 5 s, backflush time = 5 s, and 10,000 cells were collected).

Analysis of loss of fluorescence of Jurkat cells by flow cytometry: Jurkat lymphocytes (300,000 cells/mL) in complete media were aliquoted into 1.5 mL Eppendorf tubes (600 µL per tube before treatment). Fluorescent probes in DMSO stock solutions were added to each tube to achieve concentrations of 10 µM (0.1% DMSO) in triplicate. The resulting cells were incubated in a Big Shot III Hybridization Oven at 37 °C for 1 h. Cells were centrifuged at 2000 rpm for 2 min to pellet. The supernatant was removed by aspiration, the cell pellets were washed once with fluorophore-free media (600 µL), and the cells were resuspended in media (600 µL). Cells in media (100 µL) were removed and analyzed by flow cytometry (t = 0 min). The remaining cell suspension (500 µL) was incubated (37 °C) for an additional 30 min. Cells were centrifuged, washed, and analyzed by flow cytometry. Time points were recorded at 30, 60, 120, and 240 min. To keep the cell density constant, the media added for each round was 100 µL less than that of the previous cycle. Fluorescence was recorded on a cytoflex S flow cytometer and was normalized to the intensity observed at 0 min. Cellular fluorescence was analyzed with GraphPad Prism 9 (one phase exponential decay model).

Analysis of ROS with dihydroethidium (DHE): HeLa cells were seeded on 8-well chambered coverslip (Ibidi IbiTreat μ-Slide, 300 μL, 20,000 cells/well) and allowed to proliferate for 16 h prior to addition of compounds. Cells were treated with pyronins **2** or **3** (2 μM, 1 h, 37 °C), followed by addition of DHE (5 μM, 1 h). Cells were washed twice with complete media (300 μL) before imaging by confocal microscopy. Cells subjected to irradiation were scanned on a Leica SPE2 confocal microscope with a 488 nm laser at 25% power. To quantify differences in nuclear fluorescence resulting from conversion of DHE to fluorescent ethidium, regions of interest (ROI) were drawn around this organelle. Mean fluorescence values were generated and analyzed with GraphPad Prism 9. Antimycin A (20 μM) was used as a positive ROS-generating control. Cells treated only with the pyronin were used to confirm that the signal from the nucleus originated only from DHE and its metabolites. As a control, we confirmed that no enhancement in nuclear fluorescence was observed when cells were treated with DHE alone and irradiated at 488 nm for 1 or 2 min.

Analysis of cytotoxicity: Cells were seeded on a 96-well plate in complete medium at 8,000 cells / 200 μL per well 16 h prior to treatment. All compounds were serial diluted in DMSO and added to complete medium to achieve a 1:1000 dilution factor (0.1% DMSO in each well). The original media was removed from all wells by aspiration and replaced with the treatment media (200 μL) at the concentrations indicated. Plates were incubated for 48 h at 37 °C and cells were analyzed in triplicate. Following this incubation period, for HeLa cells, the media was aspirated and wells were washed with PBS (phosphate-buffered saline, pH 7.4). Cells were then detached with a solution of trypsin and EDTA (50 μL) at 37 °C for 5 min followed by treatment with complete medium containing propidium iodide (3 μM, 100 μL). The total cell-count for each well was determined by flow cytometry, using a Beckman Coulter Cytoflex S flow cytometer, and populations of live cells were identified by light scattering and uptake of propidium iodide. For Jurkat lymphocytes, cells were treated with propidium iodide (3 μM) and directly counted with the Cytoflex. Counts of viable cells for each treatment in triplicate were used to generate dose-response curves. These curves were fitted by non-linear regression with an inhibitor vs. response variable slope 4-parameter model (GraphPad Prism 9) to determine IC_{50} values. Based on curve fitting, standard errors for cytotoxic IC_{50} values were ~ 10%.

General experimental section. Chemicals were purchased from Aapptec, Acros, Aldrich, Alfa Aesar, Fisher Scientific, EMD Biosciences, or TCI America and were used without further purification unless otherwise noted. Pyronin B was purchased from Combi-Blocks as the HCl salt. Solvents were purchased from Aldrich or Fisher Scientific. ^{1}H and ^{13}C NMR spectra were acquired on Avance AVIII (500 MHz) or Varian VNMRS (400 MHz) or Bruker Avance II 400 instruments. Chemical shifts (δ) are reported in ppm referenced to $CDCl_3$ (7.22 ppm for ^{1}H and 77.0 ppm for ^{13}C) or DMSO-d_6 (2.50 ppm for ^{1}H, 39.5 ppm for ^{13}C). ^{1}H coupling constants (J_{HH}, Hz) and ^{13}C coupling constants (J_{CF}, Hz) are reported as: chemical shift, multiplicity (br = broad, s = singlet, d = doublet, t = triplet, q = quartet, m = multiplet, dd = doublet of doublets, ddd = doublet of doublet of doublets, dq = doublet of quartets, dt = doublet of triplets, ddt = doublet of doublet of triplets), coupling constant, and integration. High Resolution Mass Spectra (HRMS) of synthetic compounds were obtained at the Mass Spectrometry Laboratory at the University of Kansas on a Micromass LCT Premier or at The Ohio State University using a Thermo Scientific Q-Exactive Plus Hybrid Quadrupole-Orbitrap Mass Spectrometer. Thin layer chromatography (TLC) was performed on Merck aluminum-backed (0.20 mm) silica plates (60 F-254) and visualized with a UV lamp. Flash chromatography used Silicycle silica gel (40-63 μm, 230-400 mesh) or RediSep Rf silica gel disposable flash columns (40-60 microns). Preparative HPLC was performed with an Agilent 1290 Infinity II instrument equipped with a Hamilton PRP-1 reverse phase column (250 mm length, 21.2 mm ID, 7 μm particle size) with detection of absorbance at 215 and 254 nm, and flow rate of 18.0 mL/min with a gradient run of H_2O/MeCN (containing 0.1% TFA), 9:1 to 0:100 (24 or 35 min). All non-aqueous reactions were carried out using flame- or oven-dried glassware under an atmosphere of dry argon or nitrogen. Absorbance spectra were obtained using a semimicro (1.4 mL) UV quartz cuvette (Sigma-Aldrich, Z27667-7) on an Agilent 8452A diode array spectrometer or on a 96-well plate using a BMG Labtech ClarioStar plate reader. Fluorescence spectra were acquired using a SUPRASIL ultra-micro quartz cuvette (PerkinElmer, B0631079) on a Perkin-Elmer LS55 Fluorescence Spectrometer (10 nm slit width) or on a 96-well plate using a BMG Labtech ClarioStar plate reader. Melting points were acquired using a Bibby scientific SMP10 melting point apparatus and are uncorrected. Infrared spectra (IR) were recorded with a Shimadzu GladiATR 10 Single Reflection ATR accessory. All commercial reagents and solvents were used as received unless otherwise noted. Yields are reported based on isolated material. 3,6-Bis(diethylamino)-2,7-difluoro-9*H*-xanthen-9-one (**7**),[1] 2,2',4,4',5,5'-hexafluorobenzophenone (**12**),[1] and 3,6-bis(trifluoromethanesulfonate)xanthone (**10**)[2] were synthesized as previously reported.

Synthetic procedures and compound characterization data

General procedure A

The corresponding 3,6-diaminosubstituted benzophenone (9.00 mmol), 10 M KOH (12.0 mL, 120 mmol), and DMSO (12 mL) were heated to 180 °C for 12 h. The resulting mixture was cooled to room temperature and subsequently placed in an ice bath for 1 h. The contents were further diluted with ice cold water (100 mL), and the resulting solid was collected by vacuum filtration. The crude solid was purified via recrystallization with CH_2Cl_2/hexanes.

General Procedure B

Step 1 - The corresponding 3,6-diaminosubstituted xanthone (0.314 mmol), 3.33 equivalents of borane dimethyl sulfide (1.04 mmol), and THF (5.00 mL) were added to a round bottom flask and refluxed at 70 °C until starting material was consumed by TLC. The flask was allowed to cool to room temperature, and methanol (5 mL) was added to quench the reaction. The solvent was removed under reduced pressure and the crude product was passed through a silica gel plug (25 g of silica) pretreated with CH_2Cl_2 (25 mL) / trimethylamine (2 mL) using CH_2Cl_2 / trimethylamine (0.1%) as the eluent. The solvent was removed under reduced pressure and placed under high vacuum (0.1 mmHg) to remove all residual volatiles. The resulting solid material (xanthene) is unstable and slowly decomposes to the pyronin, a process which is considerably accelerated by the use of DDQ as described in step 2.

Step 2 - The solid material from the previous step was dissolved in CH_2Cl_2 (7 mL) and treated with DDQ (0.377 mmol). The resulting mixture was stirred at 26 °C and monitored by TLC. Upon completion, 1 mL of trifluoroacetic acid was added to the reaction mixture and the resulting mixture was stirred for an additional 5 min. Volatiles were removed under reduced pressure. CH_2Cl_2 (7 mL) was added and the crude pyronin was stirred at room temperature for 1 h. The slurry was filtered under vacuum and the solid residue was washed with CH_2Cl_2 (5 mL). The filtrate was concentrated under reduced pressure. The residue was crystallized/recrystallized using toluene. During this process, the compound was vacuum filtered while dissolved in hot toluene to remove any insoluble impurities. The toluene filtrate was reheated to dissolve all solid material, slowly cooled, and allowed to stand at room temperature for 24-48 h before the pure pyronin crystals were recovered by vacuum filtration.

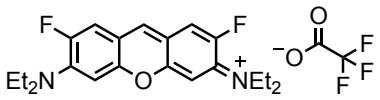

3

***N*-(6-(Diethylamino)-2,7-difluoro-3*H*-xanthen-3-ylidene)-*N*-ethylethanaminium 2,2,2-trifluoroacetate** (**2,7-Difluoropyronin B trifluoroacetate**, **3**). Using general procedure B with a reaction time of 1.5 h for step 1 and 1.5 h for step 2, xanthone **7** (synthesized from 2, 2', 4, 4', 5, 5'-hexafluorobenzophenone as previously reported[1]) was converted into pyronin **3**. Pure crystals of **3** (147 mg, 92%) were obtained. m.p. 53-55 °C; ^{1}H NMR (400 MHz, $CDCl_3$) δ 8.61 (s, 1H), 7.54 (d, *J* = 14.3 Hz, 2H), 6.93 (d, *J* = 7.4 Hz, 2H), 3.67 (q, *J* = 7.0 Hz, 8H), 1.36 (t, *J* = 7.1 Hz, 12H); ^{13}C NMR (101 MHz, $CDCl_3$) δ 160.3 (q, *J* = 38 Hz), 155.1, 150.7 (d, *J* = 253 Hz), 147.9 (d, *J* = 11 Hz), 145.4, 118.6 (q, *J* = 290 Hz, TFA), 116.4 (d, *J* = 26 Hz), 114.4 (d, *J* = 10 Hz), 99.9 (d, *J* = 5.4 Hz), 48.4, 13.2; IR (thin film) 2985, 2870, 1728, 1605, 1466, 1281, 1134, 1072 cm^{-1}; HRMS (ESI) m/z 359.1915 (M^+, $C_{21}H_{25}F_2N_2O$ requires 359.1935).

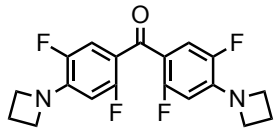

13

Bis(4-(azetidin-1-yl)-2,5-difluorophenyl)methanone (13). 2, 2', 4, 4', 5, 5'-Hexafluorobenzophenone (**12**, 2.50 g, 8.61 mmol), azetidine hydrochloride (2.34 g, 25.0 mmol), *N*,*N*-diisopropylethylamine (5.23 mL, 30.0 mmol), and acetonitrile (15 mL), were combined in a sealed tube and heated at 100 °C for 12 h. The resulting solution was concentrated under reduced pressure and the residue dissolved in CH_2Cl_2 (50 mL) and extracted with aq. HCl (1 M, 3 x 50 mL). The organic fraction was dried (anhydrous Na_2SO_4) and the solvent was removed under reduced pressure. The residue was recrystallized using CH_2Cl_2/hexane to provide 2.78 g (85%) of colorless crystals of benzophenone **13**. m.p. 155-157 °C; ^{1}H NMR (400 MHz, $CDCl_3$) δ 7.27 (dd, 2H), 5.97 (dd, *J* = 11.7, 7.1 Hz, 2H), 4.11 (td, *J* = 7.5, 2.3 Hz, 8H), 2.38 (p, *J* = 7.4 Hz, 4H); ^{13}C NMR (101 MHz, $CDCl_3$) δ 185.1, 158.6 (d, *J* = 250.1 Hz), 147.3 (d, *J* = 237.9 Hz), 143.7 (m), 117.2 (dd, *J* = 21.6, 5.1 Hz), 115.9, 99.3 (dd, *J* = 30.1, 4.2 Hz), 53.5 (d, *J* = 2.5 Hz), 17.4 (d, *J* = 2.8 Hz). IR (thin film) 2949, 2876, 1618, 1589, 1450, 1375, 1159, 895, 742 cm^{-1}; HRMS (ESI) m/z 387.1070 ($M+Na^+$, $C_{19}H_{16}F_4N_2ONa$ requires 387.1096).

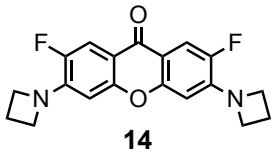

14

3,6-Di(azetidin-1-yl)-2,7-difluoro-9H-xanthen-9-one (14). Using general procedure A, benzophenone **13** was converted into **14.** After recrystallization, colorless crystals (2.68 g, 87%) of xanthone **14** were collected. m.p. 261-263 °C; ^{1}H NMR (400 MHz, $CDCl_3$) δ 7.65 (d, *J* = 12.6 Hz, 2H), 6.03 (d, *J* = 7.3 Hz, 2H), 4.13 (td, 8H), 2.43 – 2.30 (m, 4H); ^{13}C NMR (101 MHz, $CDCl_3$) δ 174.2, 153.8, 148.9 (d, *J* = 241.3 Hz), 144.4 (d, *J* = 14.1 Hz), 111.4 (d, *J* = 5.9 Hz), 111.0 (d, *J* = 20.7 Hz), 98.7 (d, *J* = 4.7 Hz), 53.5 (d, *J* = 2.6 Hz), 17.4 (d, *J* = 2.8 Hz). IR (thin film) 2953, 2884, 1618, 1530, 1464, 1352, 1252, 775 cm^{-1}; HRMS (ESI) m/z 365.1084 ($M+Na^+$, $C_{19}H_{16}F_2N_2O_2Na$ requires 365.1078).

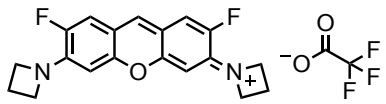

6

1-(6-(Azetidin-1-yl)-2,7-difluoro-3*H*-xanthen-3-ylidene)azetidin-1-ium 2,2,2-trifluoroacetate (**2,7-Difluoropyronin azetidine trifluoroacetate**, **6**). Using general procedure B with a reaction time of 84 h for step 1 and 4 h for step 2, xanthone **14** was converted into pyronin **6**. Pure crystals (114 mg, 76%) of **6** were obtained. m.p. > 300 °C; ^{1}H NMR (400 MHz, $CDCl_3$) δ 8.46 (s, 1H), 7.38 (d, *J* = 11.5 Hz, 2H), 6.42 (d, *J* = 7.0 Hz, 2H), 4.50 (br. s, 8H), 2.61 (q, *J* = 7.6, 6.6 Hz, 4H); ^{13}C NMR (101 MHz, $CDCl_3$) δ 160.5 (d, *J* = 37.3 Hz), 154.9, 150.3 (d, *J* = 252.3 Hz), 147.7 (d, *J* = 15.1 Hz), 145.7, 115.9 (q, *J* = 288.3, TFA), 114.8 (d, *J* = 20.5 Hz), 114.0 (d, *J* = 9.3 Hz), 96.8 (d, *J* = 5.5 Hz), 58.7, 16.9 (d, *J* = 2.9 Hz); IR (thin film) 3047, 2951, 2874, 1659, 1614, 1504, 1362, 1287, 1180, 621 cm^{-1}; HRMS (ESI) m/z 327.1292 (M^+, $C_{19}H_{17}F_2N_2O$ requires 327.1309).

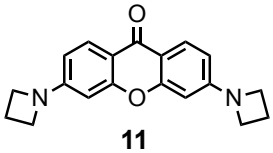

11

3,6-Di(azetidin-1-yl)-9H-xanthen-9-one (11). Acetonitrile (10 mL), KOH (10 M, 0.95 mL, 9.5 mmol), azetidine hydrochloride salt (0.936 g, 10.0 mmol), and 3,6- bis(trifluoromethanesulfonate)xanthone (**10**, 0.492 mg, 1.00 mmol)[2] were combined in a sealed tube vessel and heated to 180 °C for 12 h. Once cooled to 70 °C, the resulting slurry was filtered while hot under vacuum and the solid residue was washed with of MeOH in CH_2Cl_2 (1:9, 50 mL). The combined filtrate was concentrated under reduced pressure and the resulting residue was purified via column chromatography (3% MeOH in CH_2Cl_2 as the eluent). After removal of solvent under reduced pressure, the solid residue was recrystallized from

DMSO; the crystals were washed with cold water (50 mL) to remove trace amounts of DMSO. Colorless needle crystals of pure **11** (64 mg, 21%) were collected. m.p. 160-162 °C; ^{1}H NMR (400 MHz, $CDCl_3$) δ 8.05 (d, *J* = 8.7 Hz, 2H), 6.28 (dd, *J* = 8.7, 2.2 Hz, 2H), 6.08 (d, *J* = 2.1 Hz, 2H), 3.95 (t, *J* = 7.4 Hz, 8H), 2.37 (p, *J* = 7.3 Hz, 4H); ^{13}C NMR (101 MHz, $CDCl_3$) δ 175.0, 157.9, 155.1, 127.6, 112.4, 107.7, 95.6, 51.5, 16.4. IR (thin film) 3047, 2963, 2855, 1597, 1435, 1343, 1258, 1088, 1018, 795 cm^{-1}; HRMS (ESI) m/z 307.1458 ($M+H^+$, $C_{19}H_{19}F_2N_2O_2$ requires 307.1447).

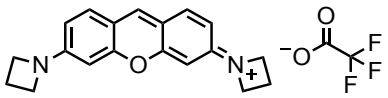

5

1-(6-(Azetidin-1-yl)-3*H*-xanthen-3-ylidene)azetidin-1-ium 2,2,2-trifluoroacetate (Pyronin azetidine trifluoroacetate, 5). Using general procedure B, the xanthene intermediate was formed after reaction for 3 h (step 1). To avoid decomposition of the final pyronin, it is imperative the xanthene intermediate is recrystallized in CH_2Cl_2/hexanes prior to step 2. The purified xanthene was converted to pyronin **5** using a reaction time of 2 h for step 2. Further purification by preparative reverse phase HPLC provided pure crystals of **5** (65 mg, 47%). m.p. 252-254 °C; ^{1}H NMR (500 MHz, DMSO-d) δ 8.66 (s, 1H), 7.80 (d, *J* = 8.9 Hz, 2H), 6.75 (dd, *J* = 8.9, 2.0 Hz, 2H), 6.46 (d, *J* = 2.1 Hz, 2H), 4.27 (t, *J* = 7.6 Hz, 8H), 2.47 (m, 4H); ^{13}C NMR (126 MHz, DMSO-d) δ 158.0 (*q*, J = 33.4 Hz, TFA), 156.9, 156.4, 146.1, 133.4, 116.5 (*J* = 296.1 Hz, TFA), 113.7, 112.5, 93.8, 51.8, 15.4; IR (thin film) 2954, 2922, 2851, 1652, 1633, 1558, 1392, 1307, 1192, 825 cm^{-1}; HRMS (ESI) m/z 291.1487 (M^+, $C_{19}H_{19}N_2O$ requires 291.1497).

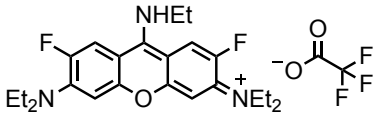

4

***N*-(6-(Diethylamino)-9-(ethylamino)-2,7-difluoro-3H-xanthen-3-ylidene)-N-ethylethanaminium 2,2,2-trifluoroacetate (9-Ethylamino difluoropyronin B, 4).** To a flame dried round bottom flask was added xanthone **7** (200 mg, 0.540 mmol). The flask was sealed and placed under a blanket of Ar. Acetonitrile (5.0 mL) was added and the resulting suspension was treated dropwise with triflic anhydride (110 µL, 0.650 mmol). The dark purple mixture was stirred for 20 min, during which all of the remaining solid solubilized. A solution of aqueous ethylamine (70% w/w, 1.00 mL, 12.6 mmol) was added dropwise. The mixture was stirred for 10 min and the resulting yellow/green solution was diluted with CH_2Cl_2 (20 mL) and extracted with H_2O (3 x 20 mL). The resulting organic fraction was dried (anhydrous Na_2SO_4) and concentrated under reduced pressure. The remaining viscous yellow oil was

passed through a plug of silica gel using CH_2Cl_2 to remove any nonpolar impurities followed by TFA:MeOH:CH_2Cl_2 (1:10:89) to elute the product. The solvent was removed under reduced pressure and the residue was crystallized using CH_2Cl_2/Hexanes to provide 237 mg of pure **4** (85%). m.p. 117-118 °C; ^{1}H NMR (400 MHz, DMSO-*d*) δ 9.54 (d, *J* = 5.9 Hz, 1H), 8.30 (d, *J* = 17 Hz, 1H), 7.94 (d, *J* = 17 Hz, 1H), 7.08-6.58 (m, 1H), 4.21–3.89 (m, 2H), 3.70–3.36 (m, 8H), 1.42 (t, *J* = 7 Hz, 3H), 1.20 (d, *J* = 7 Hz, 12H); ^{13}C NMR (126 MHz, DMSO-*d*) δ 158.1 (q, *J* = 34.5 Hz, TFA), 153.2, 152.6 (d, *J* = 333 Hz), , 149.3 (d, *J* = 178 Hz), 147.3 (d, *J* = 176 Hz), 143.8 (d, *J* = 29 Hz), 116.2 (d, *J* = 294.5 Hz, TFA), 114.8 (d, *J* = 28 Hz), 111.2 (d, *J* = 28 Hz), 101.2 (d, *J* = 316 Hz), 100.8 (d, *J* = 5.4 Hz), 46.3, 42.8, 14.2, 12.9; IR (thin film) 3303, 2984, 2941, 1616, 1500, 1198, 799 cm^{-1}; HRMS (ESI) m/z 402.2345 (M^+, $C_{23}H_{30}F_2N_3O$ requires 402.2357).

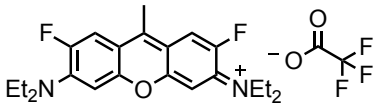

8

***N*-(6-(Diethylamino)-2,7-difluoro-9-methyl-3H-xanthen-3-ylidene)-*N*-ethylethanaminium 2,2,2-trifluoroacetate (8).** Xanthone **7** was reacted with methylmagnesium bromide solution (3.0 M) in diethyl ether at 50 °C for 15 h under argon. Further purification by preparative reverse phase HPLC provided pure crystals of **8** (28 mg, 86%). m.p. 54-56 °C; ^{1}H NMR (400 MHz, $CDCl_3$) δ 7.61 (d, *J* = 15.5 Hz, 1H), 6.96 (d, *J* = 7.7 Hz, 1H), 3.73 – 3.63 (m, 4H), 2.83 (s, 2H), 1.37 (t, *J* = 7.0 Hz, 6H); ^{13}C NMR (101 MHz, $CDCl_3$) δ 160.3 (q, *J* = 38 Hz), 155.8, 154.3, 150.7 (d, *J* = 252.5 Hz), 147.3 (d, *J* = 11.0 Hz), 113.7 (d, *J* = 9.3 Hz), 112.9 (d, *J* = 26.8 Hz), 100.1 (d, *J* = 5.4 Hz), 48.1 (d, *J* = 7.6 Hz), 14.9, 13.0; IR (thin film) 2982, 2938, 1610, 1504, 1284, 1195 cm^{-1}; HRMS (ESI) m/z 373.2084 (M^+, $C_{22}H_{27}F_2N_2O$ requires 373.2086).

NMR spectra:

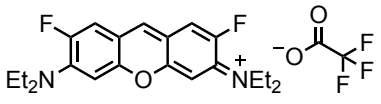

3

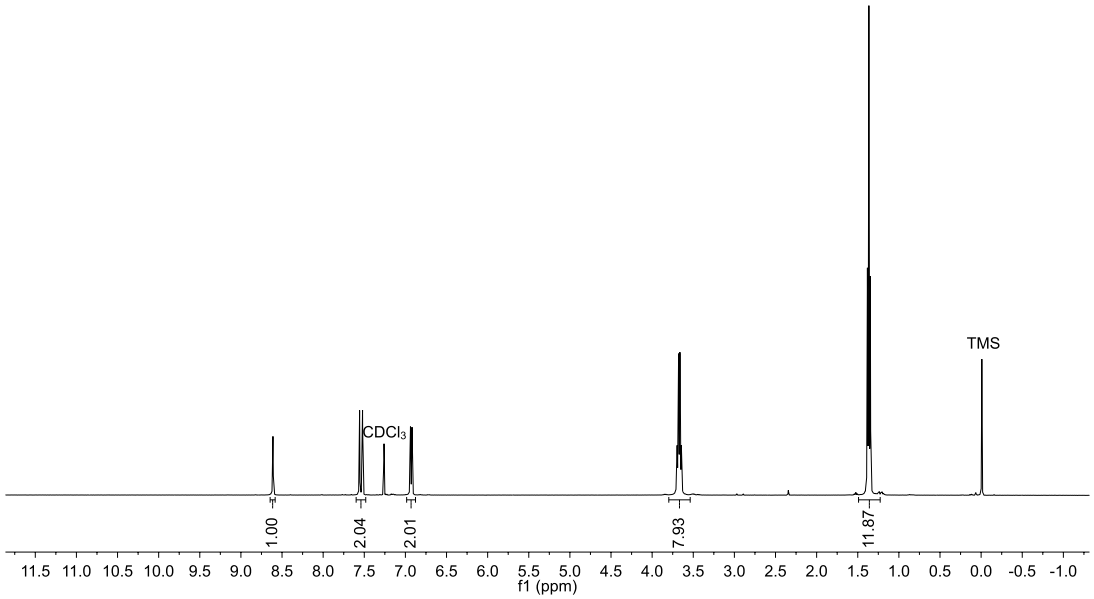

Figure S6. ^{1}H NMR (400 MHz) of **3** in $CDCl_3$.

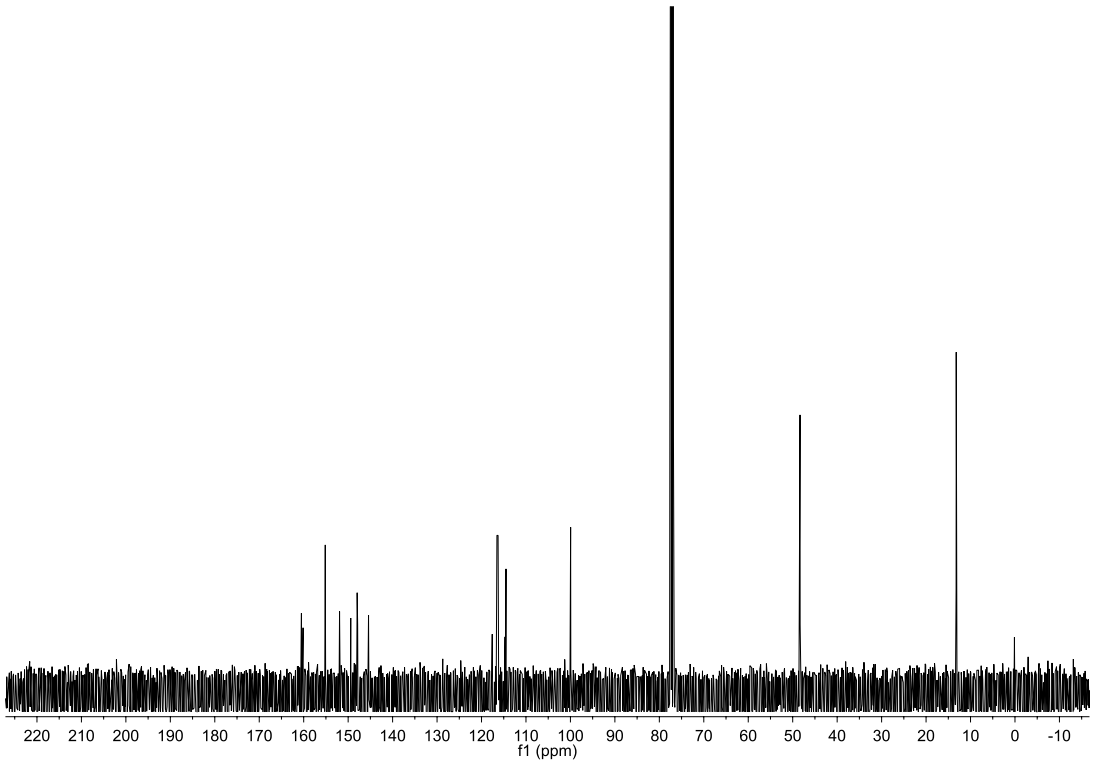

Figure S7. ^{13}C NMR (101 MHz) of **3** in $CDCl_3$.

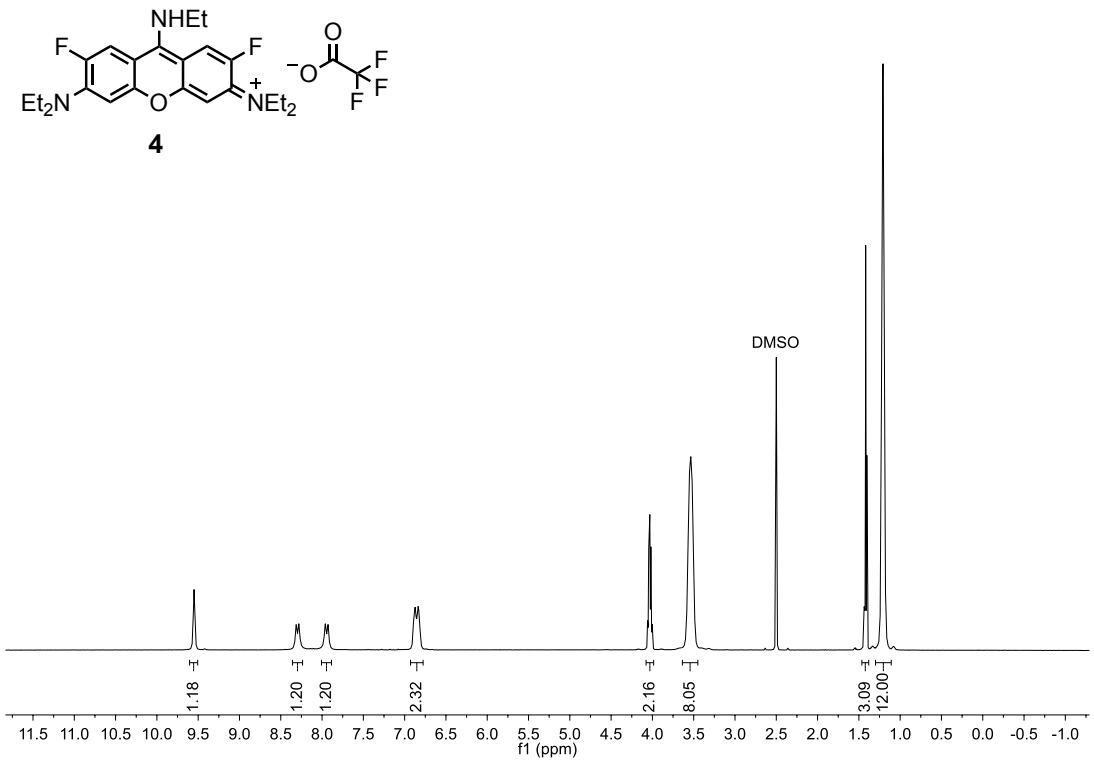

Figure S8. ^{1}H NMR (500 MHz) of **4** in DMSO-d_6.

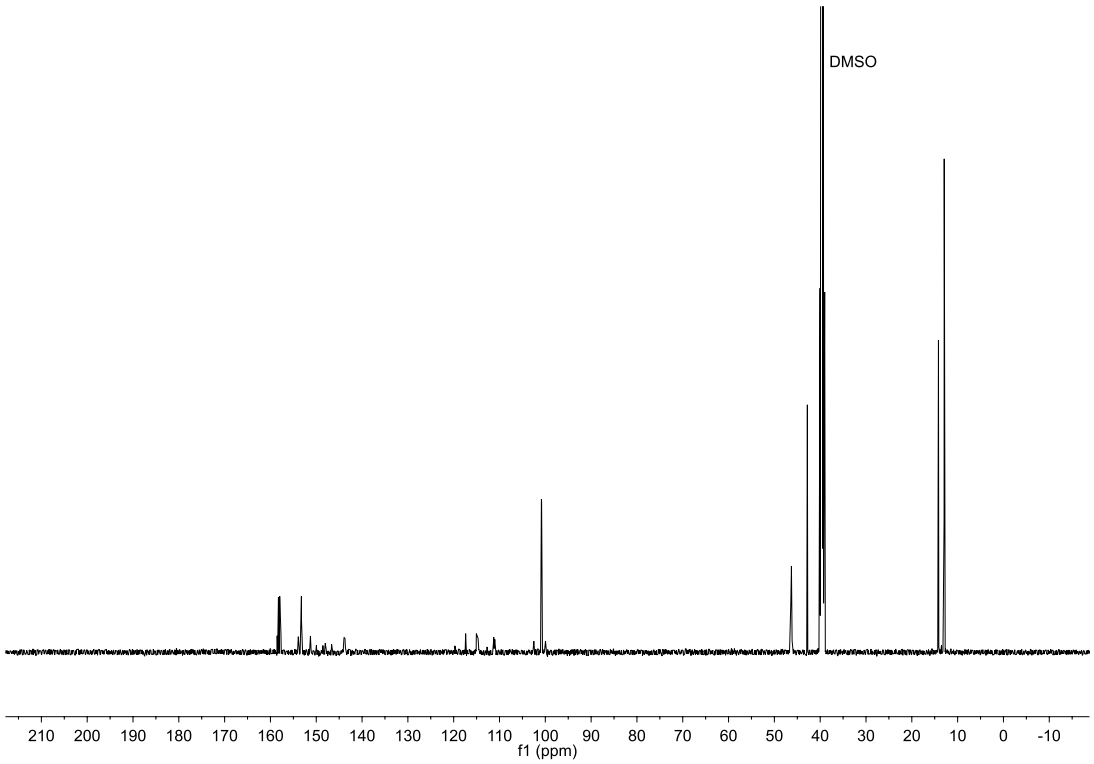

Figure S9. ^{13}C NMR (126 MHz) of **4** in DMSO-d_6.

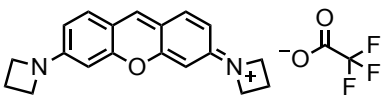

5

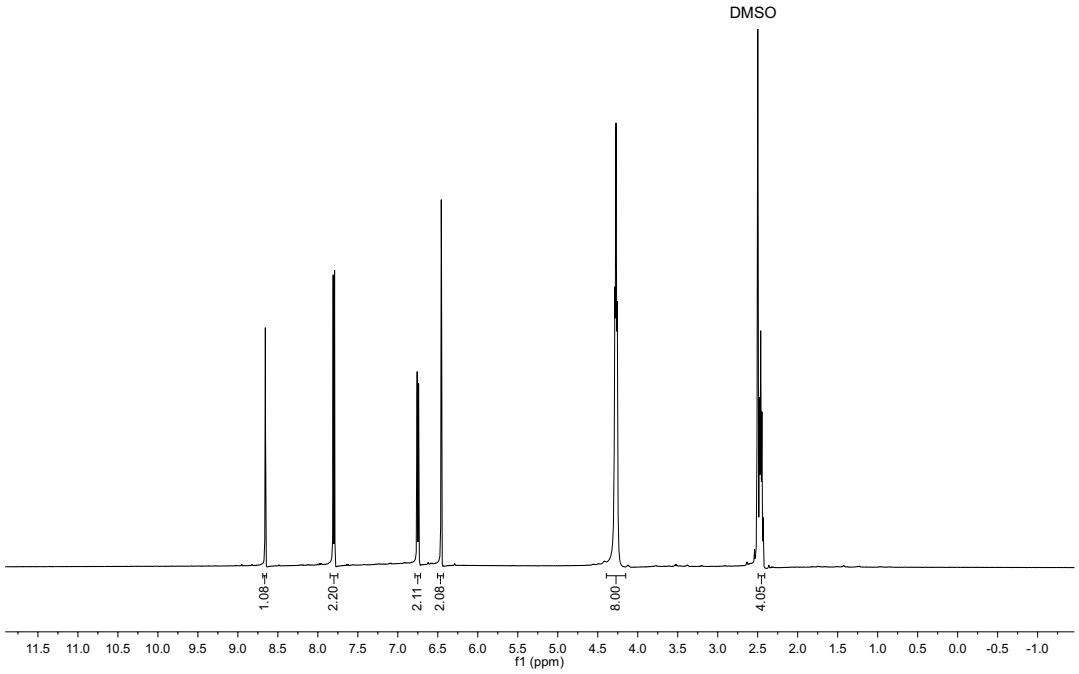

Figure S10. ^{1}H NMR (500 MHz) of **5** in DMSO-d_6.

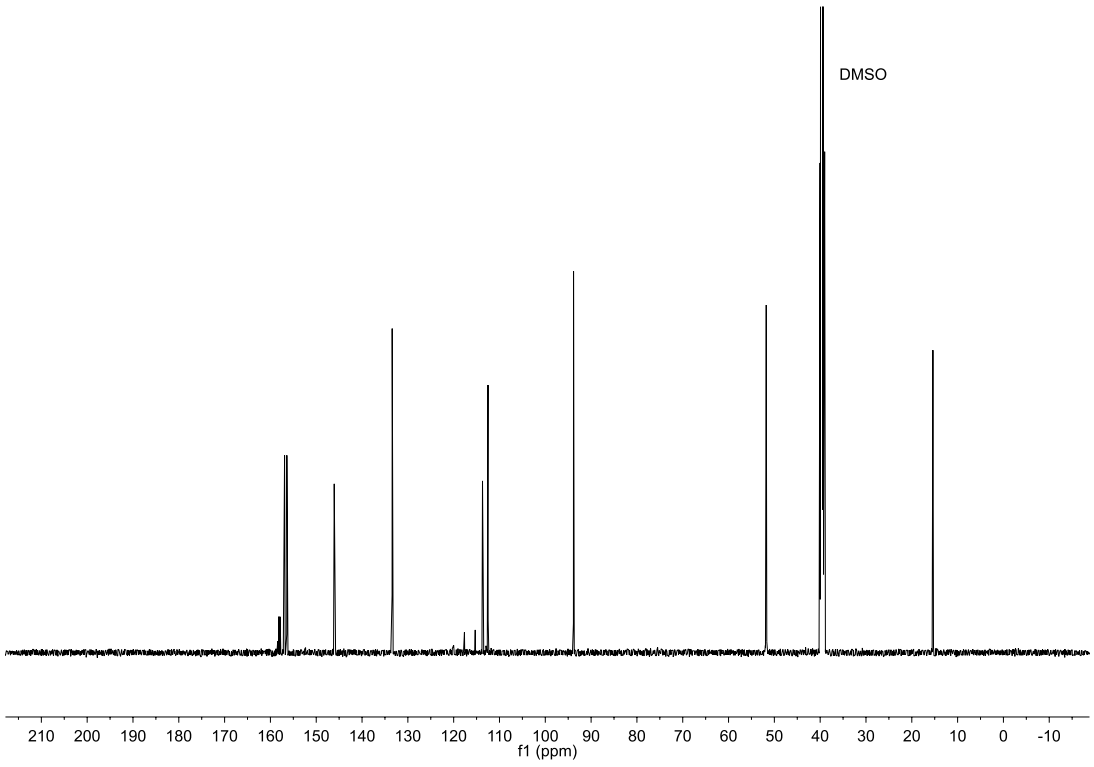

Figure S11. ^{13}C NMR (126 MHz) of **5** in DMSO-d_6.

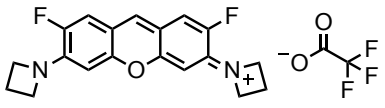

6

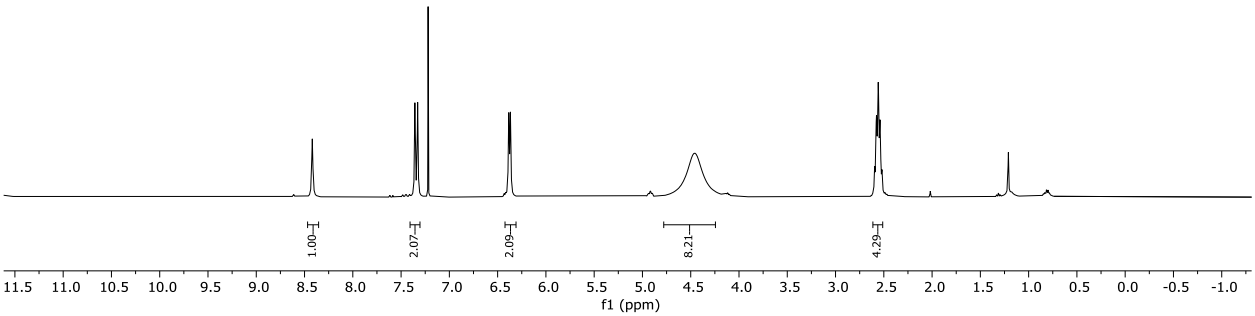

Figure S12. ^{1}H NMR (400 MHz) of **6** in $CDCl_3$.

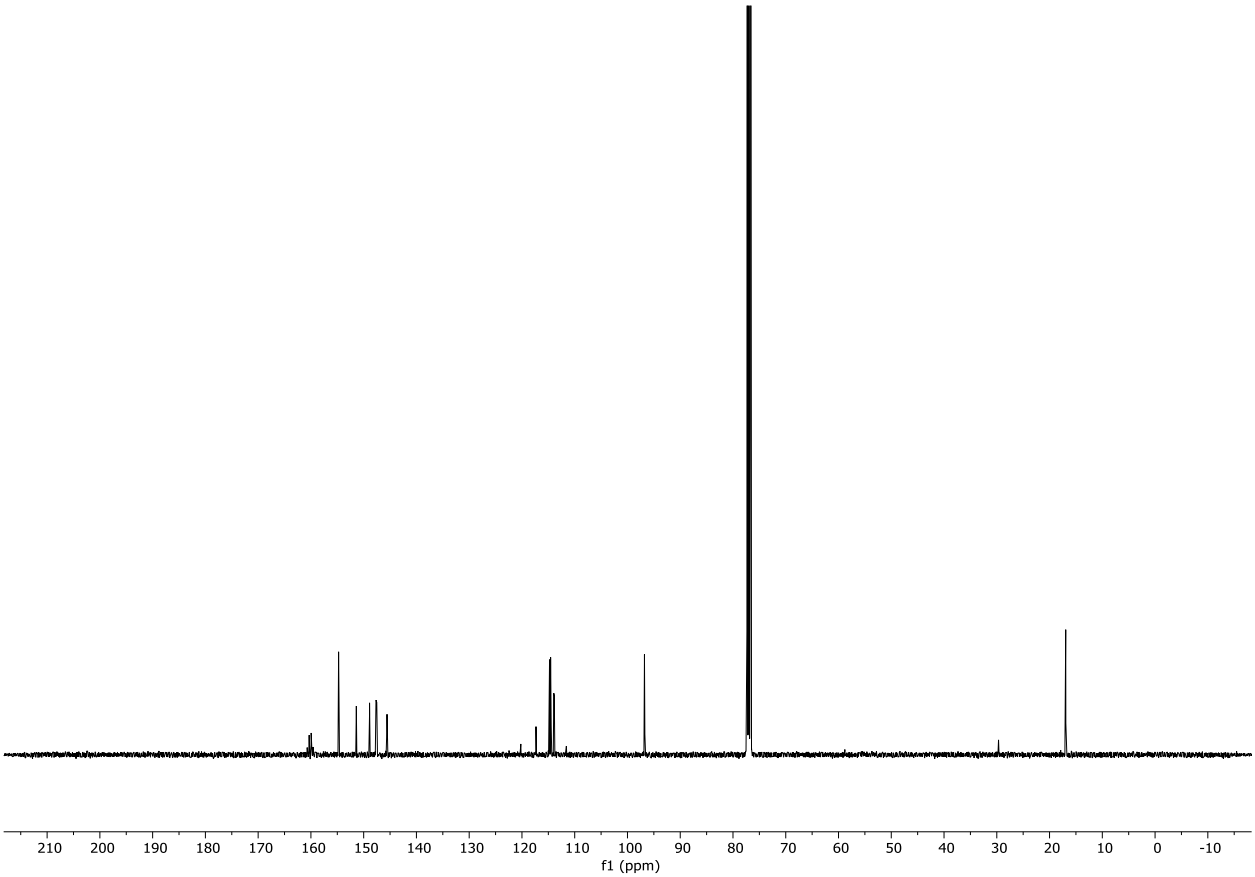

Figure S13. ^{13}C NMR (101 MHz) of **6** in $CDCl_3$.

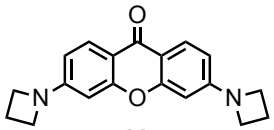

11

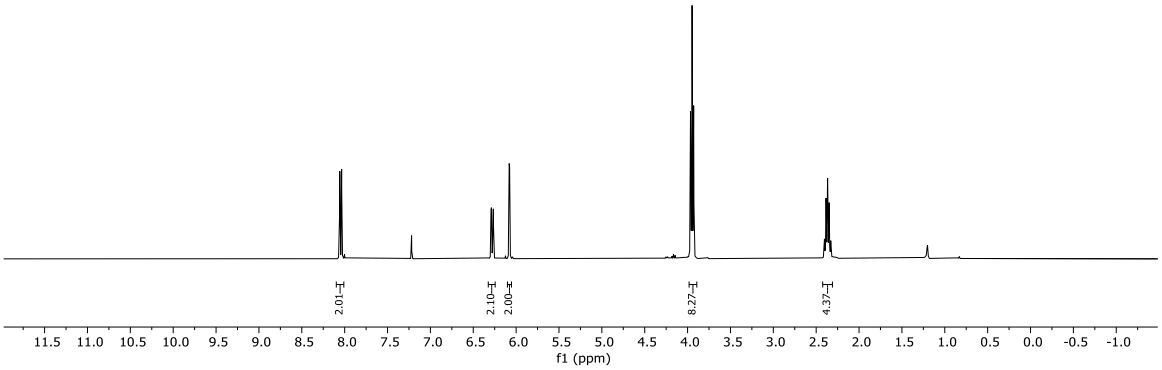

Figure S14. ^{1}H NMR (400 MHz) of **11** in $CDCl_3$.

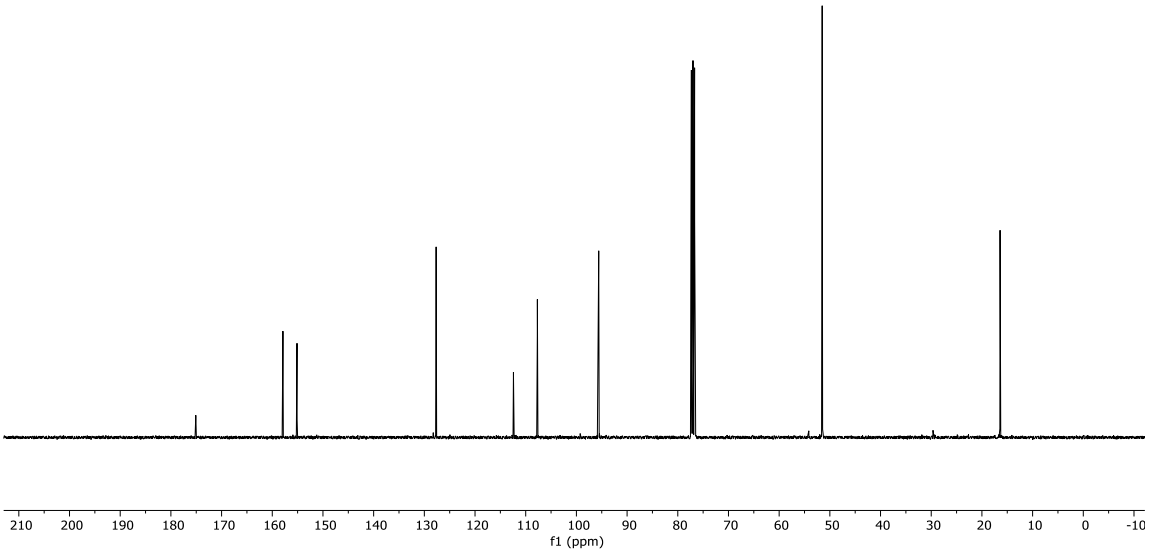

Figure S15. ^{13}C NMR (101 MHz) of **11** in $CDCl_3$.

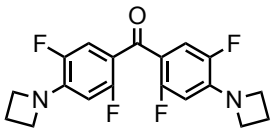

13

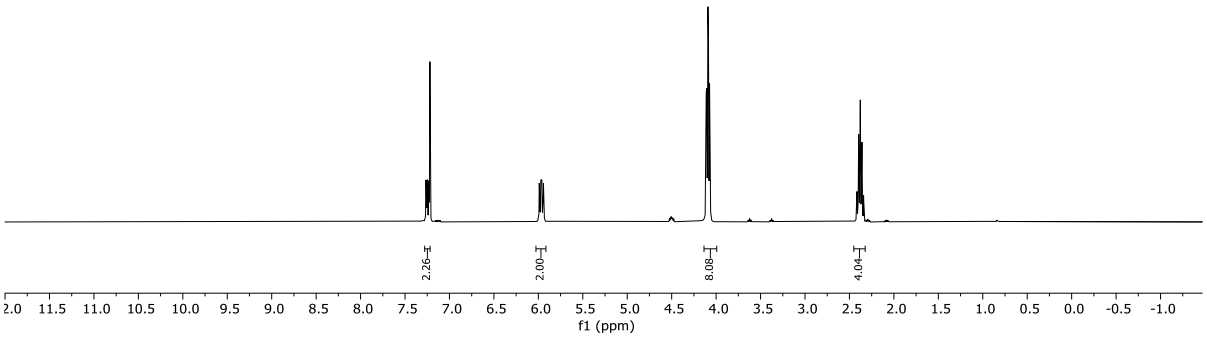

Figure S16. ^{1}H NMR (400 MHz) of **13** in $CDCl_3$

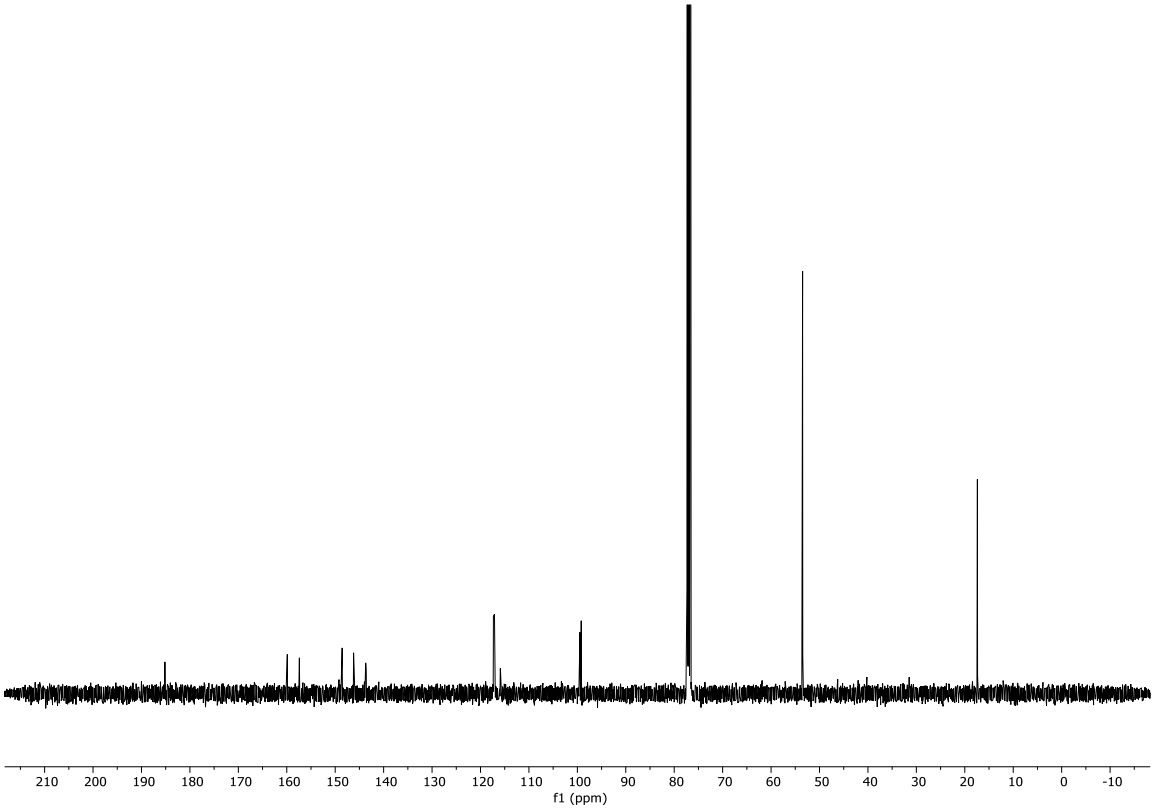

Figure S17. ^{13}C NMR (101 MHz) of **13** in $CDCl_3$.

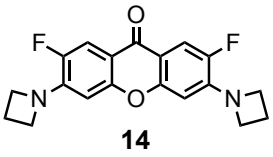

14

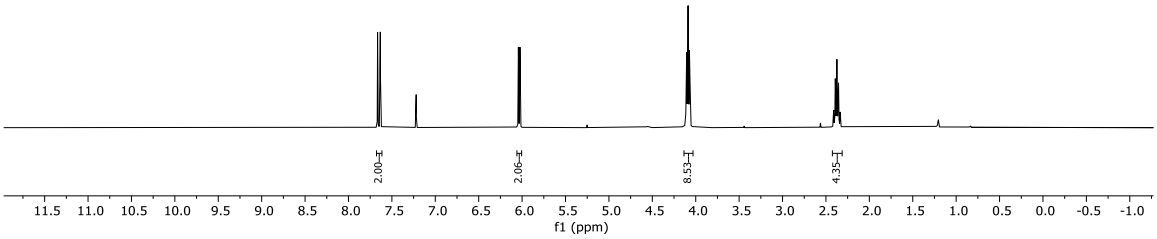

Figure S18. ^{1}H NMR (400 MHz) of **14** in $CDCl_3$.

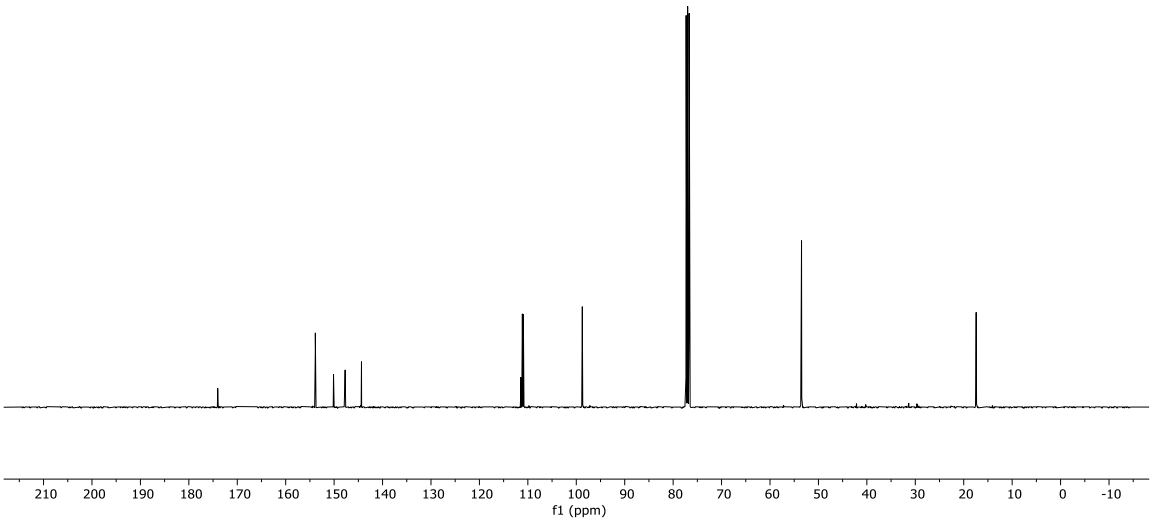

Figure S19. ^{13}C NMR (101 MHz) of **14** in $CDCl_3$.

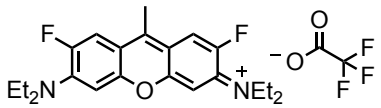

8

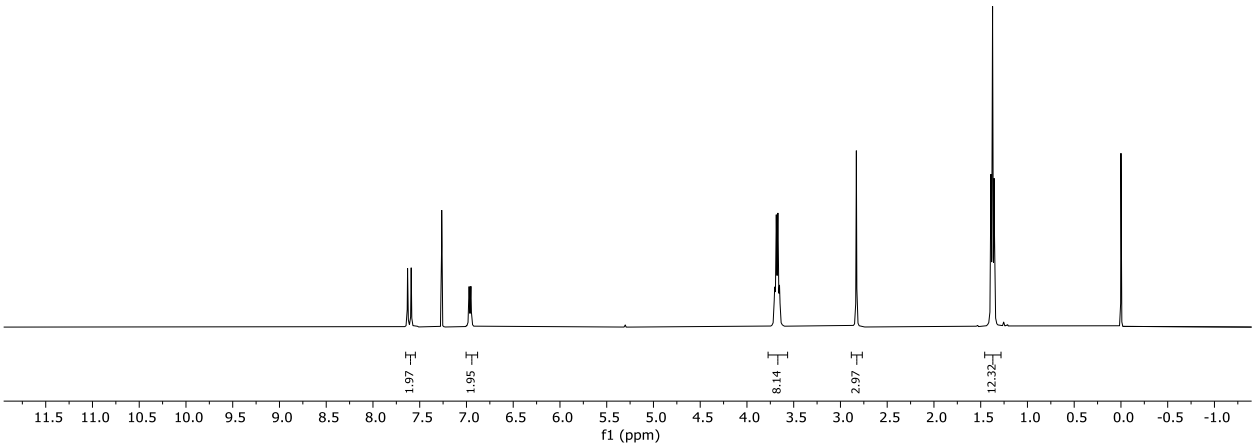

Figure S20. ^{1}H NMR (400 MHz) of **8** in $CDCl_3$.

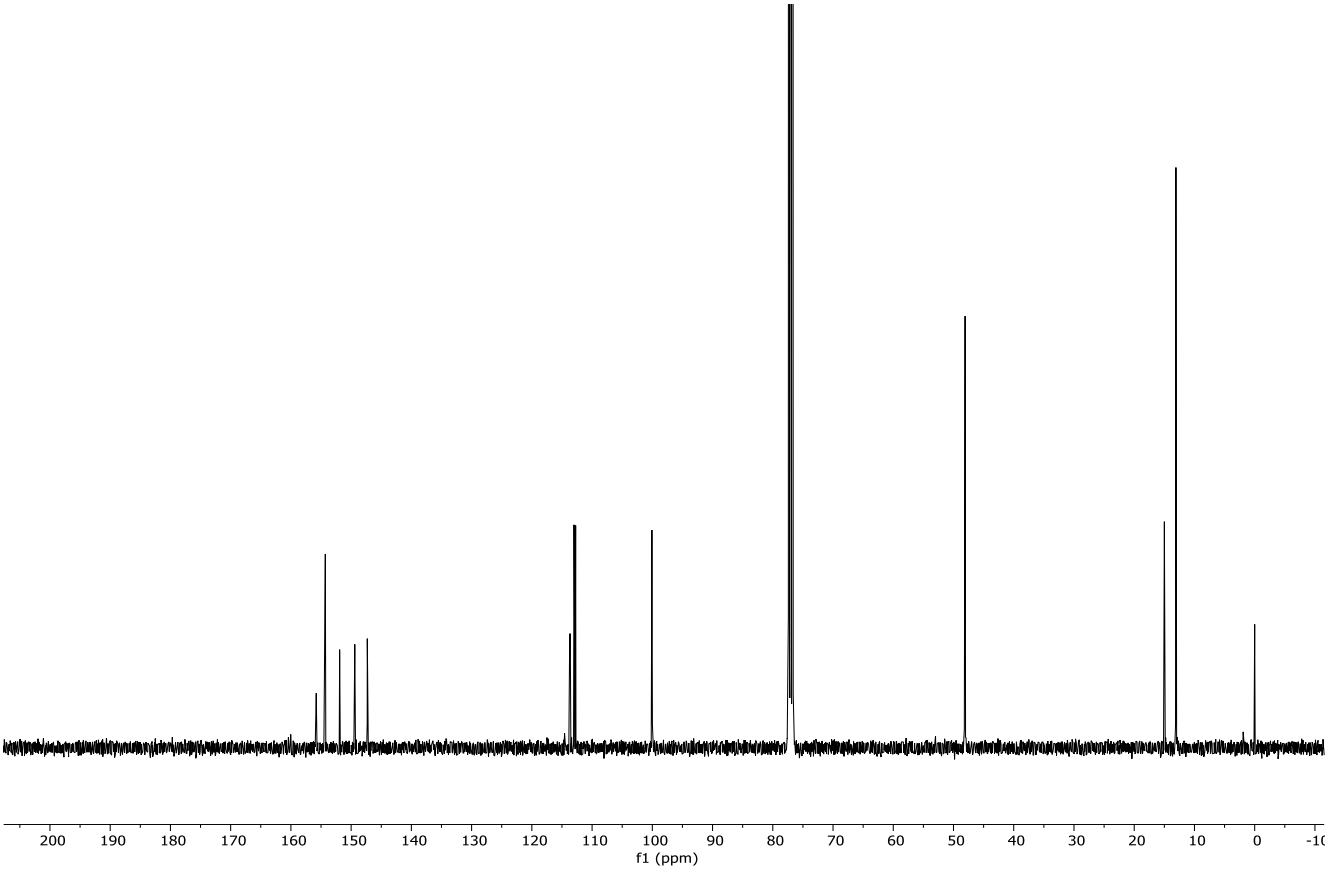

Figure S21. ^{13}C NMR (101 MHz) of **8** in $CDCl_3$.

References for the supporting information:

[1] Z. R. Woydziak, L. Fu, B. R. Peterson, *J. Org. Chem.* **2012**, *77*, 473-481.
[2] P. Stacko, P. Sebej, A. T. Veetil, P. Klan, *Org. Lett.* **2012**, *14*, 4918-4921.